Phase-Dependent Effects of a Few-Cycle Laser Pulse

D. B. Milošević,[1,2] G. G. Paulus,[3,*] and W. Becker[2,†]

[1]*Faculty of Science, University of Sarajevo, Zmaja od Bosne 35, 71000 Sarajevo, Bosnia and Herzegovina*
[2]*Max-Born-Institut, Max-Born-Strasse 2a, 12489 Berlin, Germany*
[3]*Ludwig-Maximilians-Universität, Sektion Physik, 85748 Garching bei München, Germany*

(Received 1 March 2002; published 19 September 2002; publisher error corrected 20 September 2002)

The Keldysh theory of above-threshold ionization (ATI) is applied to few-cycle laser pulses in order to explore the potential of a recently published new method to measure "carrier-envelope phase difference" phenomena. In this experiment, the carrier-envelope phase difference dependent left-right asymmetry of few-cycle ATI was measured and investigated with a correlation technique. Here, we explore spectral features of the asymmetry, present a theoretical analysis of the experiment, and establish a method to determine the duration of few-cycle pulses whose carrier-envelope phase differences are not controlled.

DOI: 10.1103/PhysRevLett.89.153001 PACS numbers: 32.80.Rm, 42.50.Hz, 42.65.Re

High-power ultrashort laser pulses with durations as short as a few optical cycles are now available as research tools [1,2] (see also the recent review article [3], and references therein). While a long monochromatic laser pulse is completely characterized by its frequency, amplitude, and polarization, a short pulse requires at least one additional parameter. Consider a short pulse with the (linearly polarized) electric field $\mathbf{E}(t) = \mathbf{E}_0(t)\cos(\omega t + \phi)$. For a given envelope $\mathbf{E}_0(t)$, the value of the phase ϕ of the carrier wave with frequency ω dramatically affects the temporal shape of the electric field. All physical processes induced by this field will depend on this "carrier-envelope phase difference" (CEPD). Therefore, its measurement and control are crucially important in a number of contexts such as coherent control, coherent soft x-ray generation, attosecond pulse generation, and particle acceleration. Carrier-envelope phase difference effects have been discussed theoretically in several papers for photoionization [4–6] and high-harmonic generation [7,8].

The current state of technology allows generation of phase-stabilized pulses in the few-cycle regime for femtosecond laser oscillators [9]. This is instrumental for frequency metrology in the optical domain [10,11]. Generally, their power is insufficient to drive strong-field effects. Amplified pulses consisting of only a few cycles are also feasible [1]. However, so far it has not been possible to stabilize their CEPD.

In a recent paper [12], it has been shown that CEPD effects can be measured, nevertheless. The method used was based on the simple fact that the angular distribution of photoelectrons loses its inversion symmetry as soon as the CEPD starts playing a role. This property can be detected by recording on a shot-to-shot basis the number of electrons emitted in opposite directions. The lack of inversion symmetry translates into an *anticorrelation* of the number of electrons flying in opposite directions, e.g., to the left and to the right. The strength of the anticorrelation mirrors the degree of influence of the CEPD. Furthermore, it can be measured as a function of electron energy, polarization, intensity, etc. Thus, the approach introduced in [12] allows a detailed investigation of CEPD effects without requiring a phase-stabilized laser. A shortcoming of the method is its sensitivity to shot-to-shot intensity fluctuations of the laser, which produce a *positive* correlation.

The purpose of this Letter is twofold: First, in the context of the strong-field approximation (SFA) [13–15], we investigate the above-threshold ionization (ATI) spectrum generated by intense few-cycle laser pulses. Based on this, second, we provide a detailed analysis of the correlation technique. Since computation of the ionization rates, which depend on the CEPD and the emission angle, is fast, it is possible to simulate the conditions of real experiments including, e.g., laser-intensity fluctuations. We are able to reproduce the results presented in [12] with remarkable accuracy. However, our calculations indicate that the pulse duration given there was slightly too short.

We assume that the laser field is switched on at some initial time $t_0 = 0$ and that the pulse duration is T_p. We describe the laser electric field $\mathbf{E}(t)$ by a vector potential $\mathbf{A}(t)$ such that $\mathbf{A}(t) = \mathbf{0}$ for $t \leq 0$ and $t \geq T_p$. This guarantees that the electric field has no dc component. In the SFA, the matrix element for direct ionization into the final continuum state f reads (in atomic units)

$$M_{fi} = -i \int_0^{T_p} dt \langle \Phi_f^{(-)}(t) | H_L(t) | \Psi_i(t) \rangle. \tag{1}$$

Here $H_L(t) = \mathbf{r} \cdot \mathbf{E}(t)$ is the interaction with the laser field, $|\Psi_i(t)\rangle$ is the initial state of the atom, for which we take a hydrogenlike state $|\psi_0\rangle \exp(iI_p t)$ with I_p the ionization energy, and $|\Phi_f^{(-)}(t)\rangle$ is the final state of the outgoing electron, which is described by a Volkov state with momentum $\mathbf{k}_f$. We then have

$$M_{fi} = -i \int_0^{T_p} dt \langle \mathbf{k}_f + \mathbf{A}(t) | \mathbf{r} \cdot \mathbf{E}(t) | \psi_0 \rangle e^{iS_{\mathbf{k}_f}(t)}, \quad (2)$$

with

$$S_{\mathbf{k}_f}(t) = \int^t dt' \{ [\mathbf{k}_f + \mathbf{A}(t')]^2/2 + I_p \}. \quad (3)$$

The integral (2) can easily be calculated numerically as it is. However, a good deal of physical insight can be gained if one employs the saddle-point approximation, which is well applicable for strong fields. This yields

$$M_{fi}^{\mathrm{SP}} = -i \sum_s \left\{ \frac{2\pi i}{\mathbf{E}(t_s) \cdot [\mathbf{k}_f + \mathbf{A}(t_s)]} \right\}^{1/2} \times \langle \mathbf{k}_f + \mathbf{A}(t_s) | \mathbf{r} \cdot \mathbf{E}(t_s) | \psi_0 \rangle \exp[iS_{\mathbf{k}_f}(t_s)], \quad (4)$$

where the summation is over all saddle points $t = t_s$ with $0 < \mathrm{Re}t_s < T_p$ and $\mathrm{Im}t_s > 0$ that are solutions of the equation

$$\partial S_{\mathbf{k}_f}/\partial t = I_p + [\mathbf{k}_f + \mathbf{A}(t)]^2/2 = 0. \quad (5)$$

The real parts of the solutions t_s specify those times when the electron has to enter the field environment in order that its drift momentum be $\mathbf{k}_f$.

In accordance with the experiment [12], here we consider the circularly polarized laser field

$$\mathbf{E}(t) = E_0 \sin^2(\omega_p t/2)(\hat{\mathbf{e}}_x \cos\psi + \hat{\mathbf{e}}_y \sin\psi)/\sqrt{2}, \quad (6)$$

where $\omega_p = \omega/n_p$ and $\psi = \omega t + \phi$ with ϕ the CEPD. A change of this phase amounts to a rotation in the (x, y) plane.

In the strong-field limit, let us ignore for the moment the ionization energy I_p. Then, for a given orientation of the detector, i.e., for a given direction of the vector $\mathbf{k}_f$, Eq. (5) has real solutions for those times t_s when the vector $\mathbf{A}(t_s)$ is in the direction of $\mathbf{k}_f$. They are obtained by intersecting a straight line from the origin in the direction of $\mathbf{k}_f$ with the curve $\mathbf{A}(t)$. The solutions correspond to discrete values of the energy $E_{\mathbf{k}_f} = \mathbf{k}_f^2/2$. For arbitrary energies and/or $I_p \neq 0$, the solutions t_s will be complex. However, $\mathbf{A}(\mathrm{Re}t_s)$ is still approximately in the direction of $\mathbf{k}_f$.

Figure 1, in its middle column, presents parametric plots in the (x, y) plane of the vector potential corresponding to the field (6) for various values of the CEPD ϕ. We assume that the detectors are positioned in the positive and the negative x directions ("right" and "left"). Symbols mark the vector potential at those times $\mathrm{Re}t_s$ when the electron has to enter the field in order to reach the left-hand or the right-hand detector. These times are the saddle points determined from the solutions of Eq. (5) for $\mathbf{k}_f$ in the positive or the negative x direction and for $E_{\mathbf{k}_f} = 5\omega$ (corresponding to the center of the electron spectrum). Indeed, the values $\mathbf{A}(\mathrm{Re}t_s)$ are close to the positive or the negative x axis. For $\phi = 0°$, the curve traced by the vector potential is symmetric with respect to the y axis, and so are then the saddle points. Hence, the spectra recorded by the left-hand and the right-hand

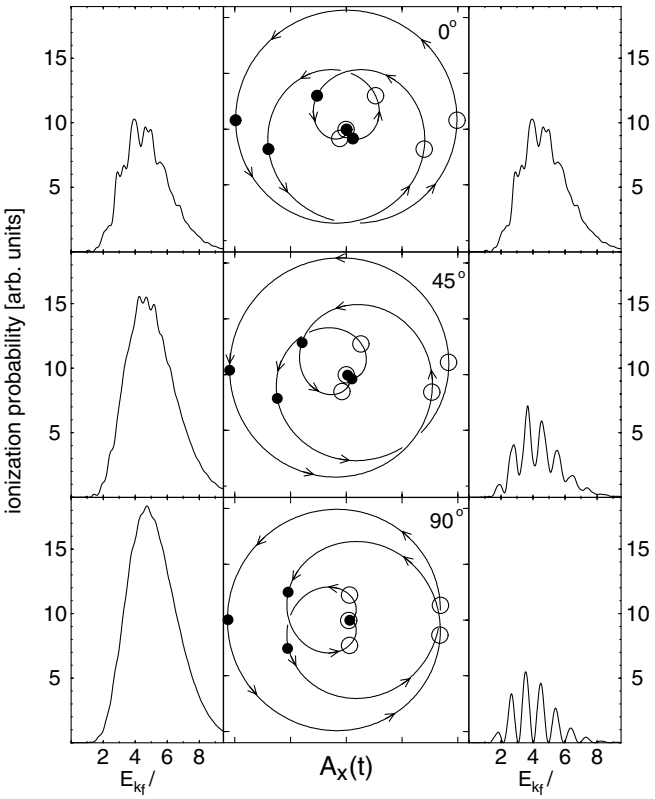

FIG. 1. Middle column: Parametric plots of the vector potential of the circularly polarized field (6) for $n_p = 4$ and the CEPDs $\phi = 0°$, 45°, and 90° from top to bottom. The arrows indicate the evolution in time. The saddle-point solutions of Eq. (5) for emission in the negative (positive) x direction are marked by solid (open) symbols. Left and right columns: Electron spectra recorded at the left and right detectors, respectively. The parameters $I_p = 14$ eV, $\lambda = 800$ nm, and $I = 5 \times 10^{13}$ W/cm^2 correspond to the experiment [12].

detectors are identical. These are displayed in the two panels to the left and to the right. They have been calculated from the matrix element (2) without the saddle-point approximation.

In general, the symmetry axis of the vector potential and, accordingly, of the saddle points is the direction $(-\sin\phi, \cos\phi)$, and the spectra observed at the right-hand and the left-hand detectors (in the positive and the negative x directions) are different. For $\phi = 90°$, the right-hand spectrum receives its dominant contributions from *two saddle points* with equal field amplitudes $|\mathbf{A}(t_s)|$, one from the leading edge and the other from the trailing edge of the pulse. The spectra depicted show that this is sufficient to generate an ATI spectrum with maximal contrast (whose spatial analog is the two-slit spectrum). In contrast, the left-hand spectrum is mostly generated by the *one saddle point* that corresponds to the very peak of the vector potential. At this time, the electric field is very close to its maximum, too. This is reflected in a spectrum that is featureless and has a high yield. The two additional saddle points for which

$A_x(\mathrm{Re}t_s) \approx -0.5$ leave no visible trace in the spectrum, owing to the highly nonlinear character of the ionization process. The CEPD $\phi = 45°$ is an example of an intermediate case: we still observe a nearly featureless spectrum at the left detector and well-resolved ATI peaks at the right detector with, however, reduced contrast. Again, this behavior can be understood from the saddle points indicated in the middle panel.

The massive left-right asymmetry—well-resolved peaks in one direction versus a single hump in the opposite direction—persists up to $n_p = 6$. For $n_p \gtrsim 10$, the spectra in opposite directions are virtually indistinguishable.

Using semiclassical methods, Dietrich *et al.* [6] calculated energy-integrated ionization rates for two opposite directions. The contrast of the left-right asymmetry was defined as the maximum ratio of the yields emitted in the two opposite directions as a function of the CEPD. Here, we can calculate this quantity as a function of the electron energy. The result is that the contrast increases with electron energy and exhibits modulations such that a maximum is reached between ATI peaks. The latter is very reminiscent of what has been predicted by Cormier and Lambropoulos [4] for cesium at 10^{10} W/cm^2. However, the explanation here is different: The modulation is due to different ATI-peak widths for different emission angles. Spectra observed under emission angles where fewer cycles contribute show broader ATI peaks than spectra under the opposite emission angle where more cycles contribute, cf. the extreme case shown in Fig. 1 for $\phi = 90°$. Consequently, the ratio of these two spectra displays a modulation. For slightly longer pulses, peak structure is observed for all emission directions. Then, in addition, the energy positions of the ATI peaks are shifted according to the different field strengths in different directions. The physics underlying our results is most closely related to the phase dependence of two-color $(\omega, 2\omega)$ angular-resolved ATI spectra [16].

In order to model the experiment of Ref. [12], first we use Eq. (2) to calculate ATI spectra corresponding to emission in opposite directions for CEPDs between 0° and 360° in steps of 1°. Next, we mimic individual laser shots by randomly choosing corresponding CEPDs ϕ. The numbers of electrons emitted to the left and to the right are proportional to the integrals over the corresponding ATI spectra. Shot noise is simulated by multiplication of these integrals with random numbers following a Poissonian probability distribution. Finally, the results are multiplied by a constant such that a given mean number of electrons per shot is achieved.

We assume a uniform distribution of the carrier-envelope phase difference because phase stabilization for amplified few-cycle pulses is not possible so far, and the time between two consecutive pulses is so long that no correlation from pulse to pulse can be expected. The assumption of a Poissonian distribution for modeling the shot noise is natural as the atoms in the laser focus do not influence each other and double ionization plays no role. Analogous to the experiment, 200 000 laser pulses are simulated. In a plot, where the two coordinate axes correspond to the number of electrons emitted to the left and the right, each laser shot then yields one entry (correlation or contingency map). The pixels of this map are colored according to the number of the corresponding events. In such a representation, anticorrelations show up in structures perpendicular to the main diagonal. In fact, this can be observed in Fig. 2. There, the simulation was repeated for pulses of various duration (four to seven cycles total width). The degree of anticorrelation strongly decreases with increasing pulse duration, as expected.

Anticorrelation can be quantified with several types of algorithms. Particularly useful are nonparametric types because they do not make any assumptions about probability distributions. One example is Kendall's τ [17], which we use in the following. Kendall's τ is defined such that positive values indicate correlation and negative values anticorrelation. The limiting cases $\tau = 1$ and $\tau = -1$ mean perfect correlation and anticorrelation, respectively. Accordingly, the contingency maps presented in Fig. 2 correspond to negative values of τ, which approach zero as the pulse duration increases. Evidently, τ is also dependent on the mean number of electrons registered per laser shot, as shot noise becomes less important the more electrons are recorded per shot. In the limit of infinitely many electrons per shot, τ would be equal to -1.

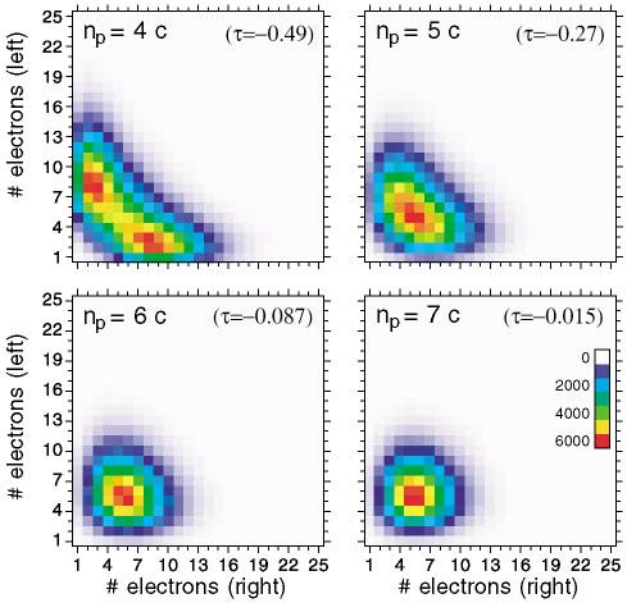

FIG. 2 (color). Contingency maps for pulses with $n_p = 4, 5, 6, 7$ for the parameters of Fig. 1. The strength of anticorrelation, for which τ is a measure, strongly depends on the pulse duration. Seven-cycle pulses (9.1 fs) yield an almost circular distribution, i.e., no appreciable anticorrelation, whereas four-cycle pulses (5.2 fs) give rise to a distribution strongly elongated along the antidiagonal. An intensity of 5×10^{13} W/cm^2 and an ionization potential of 14 eV were used.

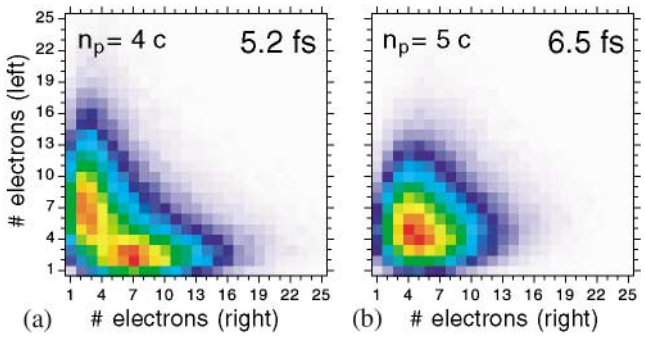

FIG. 3 (color). Contingency maps for pulses with a FWHM laser pulse duration of (a) 5.2 and (b) 6.5 fs and 4% intensity fluctuations. The other conditions are the same as for Fig. 2.

Therefore, τ can only serve as a measure of the effect of the CEPD if the number of electrons per shot is kept constant.

The disadvantage of the correlation technique in the stereo-ATI experiment is its sensitivity to laser-intensity fluctuations. These cause (positive) correlations as a pulse with higher intensity leads to a higher emission probability in both directions and vice versa. In order to investigate the consequences, we repeat the simulation described above, now allowing for intensity fluctuations. The intensity is assumed to have a Gaussian distribution, which is justified as long as the measurement time is so short that long-term drifts are negligible. The calculation of the ATI spectra was repeated for 4.75×10^{13} W/cm^2 and 5.25×10^{13} W/cm^2, and the spectra for all other intensities were obtained by interpolation. Figure 3 presents the result for pulses with durations of 5.2 and 6.5 fs. We assumed 4% pulse intensity fluctuation, which is in agreement with the experimental conditions. For Fig. 3(b) (6.5 fs), the appearence of the contingency map and the strength of the anticorrelation are very similar to the results presented in Ref. [12]. Also, Kendall's tau ($\tau = -0.03$) is close to that calculated for the experiment, although its statistical significance is higher for the simulation.

In contrast, the result for 5.2 fs [Fig. 3(a)] is clearly different and $\tau = -0.3$. Thus, by simple inspection of the contingency maps, it is possible to estimate the duration of the few-cycle pulse. In our case, we obtain a value of 6.5 fs, i.e., longer than estimated on the basis of autocorrelation. Although intensity fluctuations affect the outcome of a stereo-ATI experiment, it is possible to account for the corresponding effects.

In conclusion, we applied Keldysh theory to few-cycle pulses. The lack of inversion symmetry of the field leads to a pronounced left-right asymmetry of the angular-resolved photoelectron spectrum. The theory was shown to reproduce recent experimental data and to generate a clear signature of the pulse length.

D. B. M. gratefully acknowledges support by the VolkswagenStiftung.

*Also at MPI for Quantum Optics, 85748 Garching bei München, Germany.
†Also at Center for Advanced Studies, Department of Physics and Astronomy, University of New Mexico, Albuquerque, NM 87131.

[1] M. Nisoli *et al.*, Opt. Lett. **22**, 522 (1997).
[2] F. Krausz, Phys. World **14**, 41 (2001).
[3] T. Brabec and F. Krausz, Rev. Mod. Phys. **72**, 545 (2000).
[4] E. Cormier and P. Lambropoulos, Eur. Phys. J. D **2**, 15 (1998).
[5] I. P. Christov, Opt. Lett. **24**, 1425 (1999).
[6] P. Dietrich, F. Krausz, and P. B. Corkum, Opt. Lett. **25**, 16 (2000).
[7] A. de Bohan, Ph. Antoine, D. B. Milošević, and B. Piraux, Phys. Rev. Lett. **81**, 1837 (1998); A. de Bohan, Ph. Antoine, D. B. Milošević, G. L. Kamta, and B. Piraux, Laser Phys. **9**, 175 (1999).
[8] F. Krausz, T. Brabec, M. Schnürer, and C. Spielmann, Opt. Photonics News **9**, 46 (1998); G. Tempea, M. Geissler, and T. Brabec, J. Opt. Soc. Am. B **16**, 669 (1999).
[9] A. Apolonski *et al.*, Phys. Rev. Lett. **85**, 740 (2000).
[10] J. Reichert *et al.*, Opt. Commun. **172**, 59 (1999).
[11] D. J. Jones *et al.*, Science **288**, 635 (2000).
[12] G. G. Paulus *et al.*, Nature (London) **414**, 182 (2001).
[13] L. V. Keldysh, Zh. Eksp. Teor. Fiz. **47**, 1945 (1964) [Sov. Phys. JETP **20**, 1307 (1965)]; F. H. M. Faisal, J. Phys. B **6**, L89 (1973); H. R. Reiss, Phys. Rev. A **22**, 1786 (1980).
[14] V. S. Popov, Pis'ma Zh. Eksp. Teor. Fiz. **73**, 3 (2001) [JETP Lett. **73**, 1 (2001)].
[15] G. L. Yudin and M. Yu. Ivanov, Phys. Rev. A **64**, 013409 (2001).
[16] D. W. Schumacher and P. H. Bucksbaum, Phys. Rev. A **54**, 4271 (1996); a review of two-color effects has been given by F. Ehlotzky, Phys. Rep. **345**, 175 (2001).
[17] W. P. Press, B. P. Flannery, S. A. Teukolsky, and W. T. Vetterling, *Numerical Recipies* (Cambridge University Press, Cambridge, 1986).